PHYSICAL REVIEW B **78**, 081405(R) (2008)

Efficient sticking of surface-passivated Si nanospheres via phase-transition plasticity

M. Suri and T. Dumitrică*
Department of Mechanical Engineering, University of Minnesota, Minneapolis, Minnesota 55455, USA
(Received 27 July 2008; published 26 August 2008)

Large-scale atomistic simulations considering a 5 nm in radius H-passivated Si nanosphere that impacts with relatively low energies onto a H-passivated Si substrate reveal a transition between two fundamental collision modes. At impacting speeds of less than ~1000 m/s *particle-reflection* dominates. At increased speeds the partial onset in the nanosphere of a β-tin phase on the approach followed by *a*-Si phase on the recoil is an efficient dissipative route that promotes *particle capture*. In spite of significant deformation, the integrity of the deposited nanosphere is retained. Our result explains the efficient fabrication of nanoparticulate films by hypersonic impaction, where the nanoparticle impact velocities equal 1000–2000 m/s.

DOI: 10.1103/PhysRevB.78.081405 PACS number(s): 82.20.Wt, 62.25.−g, 62.50.−p

The fundamental understanding of the nanoparticle-surface collision modes in the low-energy regime (of less than ~1 eV/atom) is of considerable importance because achieving efficient sticking to surfaces with preservation of a grainy structure are key issues for creating new materials. Nanoparticle production in the gas phase, coupled with the application of chemical coatings and the deposition onto substrates, is a combination of aerosol technologies used for manufacturing novel nanostructured surfaces and thin films.[1–6] Chemical passivation in the gas phase is essential for preventing coalescence and large particle growth but makes the deposition step challenging. Deposition strategies have been developed, some necessitating the creation of defects in the substrate in order to pin the impinging nanoparticles,[1] which otherwise would be reflected. Remarkably, impact in the newly available regime of 1000–2000 m/s speeds leads to efficient capturing of nanoparticles as small as 2 nm in radii[5,6] made of various combinations of elements (Si, C, and N) and without prior substrate treatments.

The achieved deposition of the well-studied surface-coated Si nanospheres,[7] as demonstrated by the produced dense particulate films,[5,6] has been especially puzzling for a number of reasons: (i) In macrosphere-surface impact, inelastic behavior is usually due to the nucleation of dislocations,[8] which serves as a contact-stress release mechanism. At the nanoscale this mechanism is unlikely to operate due to both the small time and size scales. Indeed, the impact duration (τ) can be estimated with the classical Hertz theory[8] applied to a nanosphere-plane collision. One obtains picosecond durations for τ, which means that the nanosphere experiences very high strain rates. As indicated by molecular-dynamics (MD) investigations, under such extreme conditions nanomaterials are exhibiting new behaviors. For example, a high-rate compression of metallic nanowires creates amorphization[9] rather than dislocations. Furthermore, it is also accepted that even under slower applied strain rates, dislocations cannot be accommodated in nanoparticles with dimensions below a critical size. Supporting this point, recent MD (Ref. 10) obtained that bare Si nanospheres experience a first-order phase transition under severe compression. (ii) The Si nanospheres have been mechanically compressed with a nanoindentor tip and were found superhard,[7] i.e., very large pressures, up to four times larger than in bulk were needed to generate yield. Thus, any plastic mechanism requires high contact pressures and it is not known whether such pressures are generated during hypersonic impaction. Finally (iii), the surface chemistry plays an important role as strong adhesion promotes sticking. In the ideal case, previous MD obtained that bare Si nanospheres are always captured by the bare Si substrate due to the strong covalent bonding.[11] However, the formation of new Si-Si bonds is hindered when chemically passivated contacts are involved. For example, MD obtained that the coalescence of Si nanoparticles[12] was significantly slowed down when surfaces were H passivated. Thus, a short τ inhibits adhesion and should promote particle reflection.

In summary, the practical evidence and the accumulated understanding obtained from MD studies pose the compelling question of how the surface-passivated Si nanospheres are deposited onto substrates. Using MD, here we show that under large enough impacting speeds the reduced chemical reactivity of surfaces no longer obstructs the attachment of the nanospheres. In the absence of dislocations, phase-transition plasticity provides an efficient route for dissipating the incident translational energy and changing the collision dynamics from particle reflection to particle capture.

In a series of classical MD simulations we examined the microscopic details of the collision process between a projectile Si nanosphere of 5 nm in radius (R) and a Si substrate exposing its (001) surface. The considered impacting speeds (V_0) were of less than 2000 m/s. To account for the practical conditions of reduced surface reactivity we considered fully H-coated surfaces.[13] The covalent Si-Si bonding, the surface chemistry, and the dynamical bonding between the nanosphere and substrate were described with transferable potentials based on the concept of bond order.[14–16] This family of interatomic potentials describes very well the most stable phases of Si in the absence and under external pressure, as well as the Si-H bonding, but is less suitable for describing fracture. However, the fracture of Si nanospheres was not identified experimentally.[7] Both the nanosphere, containing 31 075 Si atoms, and the substrate, containing 72 000 Si atoms, were initially equilibrated at 500 K in order to mimic the elevated temperature experimental conditions of Rao *et al.*[5] As before,[11] during collision the last two bottom layers were kept fixed in time and the substrate temperature was controlled with Langevin dynamics applied to the next ten atomic layers. All other atoms were followed with a velocity

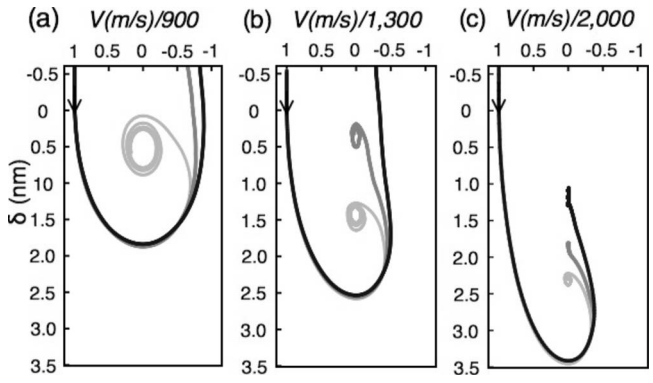

FIG. 1. Phase space trajectories for three impacting speeds: (a) 900 m/s, (b) 1300 m/s, and 2000 m/s. The nanosphere approaches the substrate with positive V, touches down at $\delta=0$, reaches $V=0$ at maximum penetration, and recoils with negative V. Arrowheads indicate the time flow.

Verlet algorithm. A time step of 0.8 fs was used for all atoms. Periodic boundary conditions were applied to the horizontal X and Y directions (the Z impact direction is vertical).

Unlike under energetic impact conditions,[17] our MD did not lead to fragmenting and spreading of the nanosphere or cratering of the substrate. Only a few H atoms were ejected under the highest V_0. The obtained collision modes can be identified in the panels of Fig. 1, presenting the phase-space trajectories for the center of mass of the impacting nanosphere under three values of V_0 and three surface-coating combinations: H-passivated nanosphere and substrate (black), H-passivated nanosphere and bare substrate (gray), and bare nanosphere and substrate (light gray). For the convenience of comparison, the instantaneous speed (V) was normalized by V_0.

On the approach stage the important parameter is V_0. The nanosphere is touching down and it advances with negative acceleration until a maximum penetration point is reached. The magnitude of V_0 is reflected in the nanosphere deformation measured when $R>Z$ by $\delta=R-Z$, where Z is the vertical positive displacement of the nanosphere center of mass measured with respect to the top of the substrate. The adhesive forces appear secondary since as in the Hertz model,[8] the nanosphere does not show accelerated motion in response to the adhesive contact forces. Additionally, under the same V_0, values for δ presented in Fig. 1 are similar for all three surface combinations considered.

On the recoil stage the outcome depends on both V_0 and the chemical reactivity of surfaces. For $V_0=900$ m/s the black and gray curves indicate that the impacting H-passivated nanosphere is reflected by both the bare and H-passivated substrate. The collision is practically elastic as V_0 restitution is as high as 80%. Our MD showed that the reflection mode, which eluded previous microscopic investigations,[11,18,19] dominates for $V_0<1000$ m/s when weakly interacting surfaces are involved. As a useful reference, the light gray curve in Fig. 1(a) indicates that under the same V_0 but larger adhesion, the bare nanosphere follows the path of a spiral sink and it is captured by the bare Si substrate. V and δ form a damped cyclic path toward the final equilibrium point, which is not reached during the shown 40 ps of MD time. Thus, energy dissipation is very slow. This mode is the previously identified soft landing,[11,18] where the deposit maintains its crystalline structure and the dissipation of the incident energy involves the substrate.

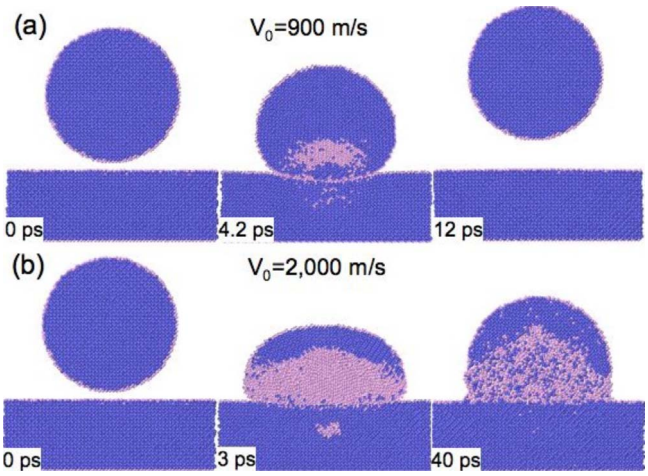

FIG. 2. (Color online) MD simulations of H-passivated Si nanosphere impacting onto a H-passivated Si substrate show two collision modes: (a) reflection and (b) capture. The middle frames show the maximum penetration instant. Only cross sectional views are shown and H atoms are not represented. The color code carries the local PE with blue (gray) and pink (light gray) representing atoms with PE absolute values larger and smaller than 4.4 eV/atom, respectively.

To our surprise, for larger V_0 a different behavior occurs: The H-passivated nanosphere impacting on the bare substrate, Fig. 1(b), and even on the H-passivated substrate, Fig. 1(c), falls into the path of a pure sink and it is captured with no oscillations. More precisely, this behavior was obtained above the critical V_0 of 1250 m/s (1580 m/s) for the impact on the bare (H-passivated) substrate. Large δ values can be noted, indicating that the nanosphere experiences significant deformation. The small V_0 restitution and the lack of vibrational contact demonstrate efficient dissipation of the incident energy. It can be also seen that the soft landing mode undergoes the same qualitative transition, which was the main finding of a previous work.[11]

The collision dynamics is further conveyed in Fig. 2. In a typical reflection the H-passivated nanosphere experiences deformation over a finite region of circular shape around the point of contact, as macroscopically expected. At maximum penetration, Fig. 2(a) (middle), there is a significant potential-energy (PE) increase only near the region of contact, as indicated by the change in color (gray level). This change appears reversible as the spherical shape is regained and the energetic differences are washed out after detachment (last frame). The capture mode, Fig. 2(b), is characterized by a severe deformation of the approaching nanosphere, which assumes at maximum penetration (middle) a domelike shape with a large contact region. There is a significant PE change in a large conical volume of height $\sim R$ and with the contact region as base. The irreversible character transpires from the PE distribution in the final configuration (last frame) and from the sphere cut out by a plane shape of the end deposit, optimal for adhesion.

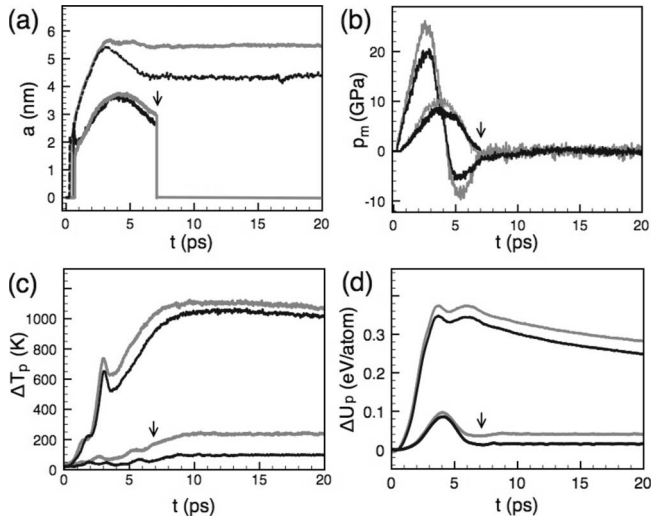

FIG. 3. Time evolution of (a) contact radius and (b) contact stress. Variation of nanosphere's (c) temperature, and (d) potential energy under two impacting speeds, V_0=900 m/s (lower two curves) and V_0=2,000 m/s (upper two curves), and two surface types, H-passivated nanosphere and substrate (black), and H-passivated nanosphere and bare substrate (gray). Down arrows mark the particle release instants.

Adhesion is quantified geometrically in Fig. 3(a), which presents the time evolution of the contact radius (a) under the two collision modes. During approach a increases and reaches its maximum at the maximum penetration instant, regardless of the surface chemistry. The final a value depends on both V_0 and the surface chemistry. Focusing on the capture mode, we see that a decreases during the recoil, most significantly when both the nanosphere and substrate are H passivated. Even in this case the final a is large, comparable with R. Adhesion was next quantified by the finite adhesion energy (γ_a), defined as the bonding energy measured per contact area, between the atoms of the nanosphere and those of the substrate. We obtained 0.07 and 0.03 eV/Å^2 for the H-passivated nanosphere impacting on the bare and H-passivated substrate, respectively. For comparison, γ_a =0.1 eV/Å^2 when bare Si surfaces are involved. Thus, it appears that the capture occurs without substantial support from the adhesive contacts. Another observation of interest is that after approach, γ_a is not changing notably because of the large number of H atoms trapped in the contact region.

Figure 3(b) shows the mean distributed contact stress (p_m), computed as the net vertical force acting on the nanosphere divided by the instantaneous contact area πa^2. Our recorded data show that significant pressures are reached during impact, sufficient to produce yield according to experimentation.[7] Interestingly, p_m vanishes after the collision not only in the reflection but also in the capture mode. In the latter, it indicates the occurrence of a stress-relieving transformation.

During collision the incident energy is converted into internal degrees of freedom, producing temperature (ΔT_p) and PE (ΔU_p) changes in the nanosphere. Examination of the energy flow confirms the large dissipation in the capture mode. In Fig. 3(c) the large ΔT_p shows that the particle heats

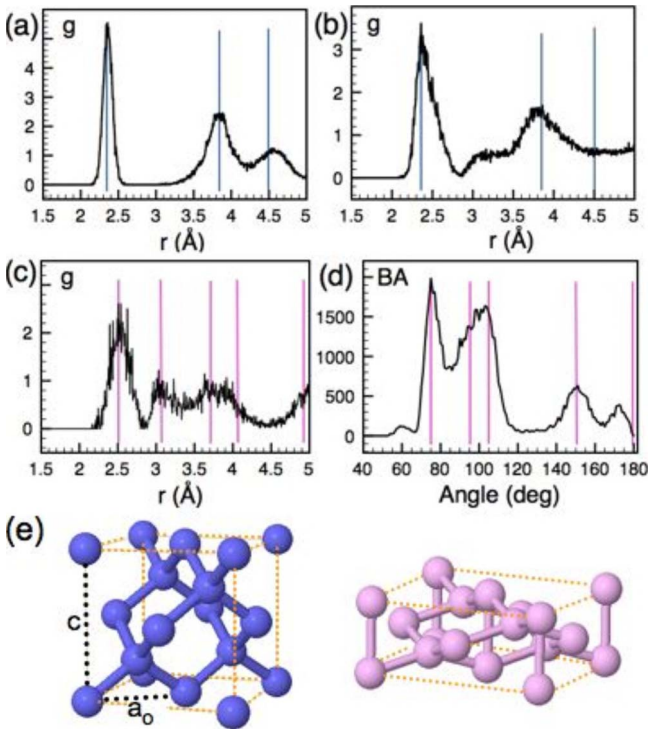

FIG. 4. (Color online) Pair-correlation function of the H-passivated Si nanosphere at maximum penetration for (a) V_0 =900 m/s and (b) V_0=2000 m/s. Vertical bars mark the neighbor position in cubic Si. (c) Pair-correlation and (d) bond-angle distributions in the most deformed conical region. Vertical bars mark neighbor positions and bond angles in bulk β-tin Si. (e) Unit cells for cubic diamond (left) and β-tin Si (right).

up during and after the 2000 m/s collision and thus a large amount of the incident energy is irreversibly transferred into thermal agitation. Figure 3(d) demonstrates the occurrence of a plastic change since after collision there is a significant PE difference with respect to the original crystalline state.

To identify the nature of this plastic change causing ΔT_p and ΔU_p rises, we monitored the nanosphere structure by computing its pair-correlation function (g). Particularly revealing were investigations at the maximum penetration instant, presented in Fig. 4. On one hand, under V_0 =900 m/s Fig. 4(a) indicates that the cubic Si structure is maintained, as the main peaks are well centered on the neighbor position in cubic Si, where each atom bonds to four other equivalent atoms in an undistorted tetrahedral pattern, Fig. 4(e) (left). On the other hand, under V_0=2000 m/s Fig. 4(b) shows the presence of a new structural arrangement other than cubic Si. Indeed, there is a widening and simultaneous decrease in the main peak height, as well as the appearance of a new peak at the interatomic distance (r) of ~3 Å. For more insight, we focused on the conical volume with high PE indicated in Fig. 2(b) (middle), where we found 5500 sixfold coordinated Si atoms with bond lengths that did not exceed 2.8 Å. In addition to g, we computed the bond-angle (BA) distribution. These results prove that the dominant structural changes correspond to a β-tin phase of Si, shown in Fig. 4(e) (right). This new phase is derived from the cubic Si by flattening the tetrahedral grouping to the

extent that two other atoms are brought into close proximity, which increases the coordination from 4 to 6. Indeed, in Fig. 4(c) g has two sharp peaks at 2.5 and 3.1 Å, which match very well the first- and second-neighbor distances of β-tin Si. All BAs are 109° in cubic Si. However, in Fig. 4(d) they are grouped around the five distinct BA of the β-tin.

On the basis of this key observation, the observed reflection to capture transition is interpreted as follows. On the approach stage, nanosphere-substrate adhesion occurs due to the new Si-Si covalent bonds formed in the contact region. For $V_0 < 1000$ m/s, these bonds rupture under the vigorous backward motion caused by the largely reflected incident energy. However, for $V_0 > 1000$ m/s, in the absence of dislocation, the atomic rearrangement caused by a displacive phase change represents the next available gateway for absorbing irreversibly a significant amount of the incident energy. Having a smaller crystallographic c/a_0 ratio (0.55 with $a_0 = 4.73$ Å) than cubic diamond (1.42 with $a_0 = 3.82$ Å), the β-tin phase has geometric advantage as it simultaneously relieves the compressional stress and augments the contact area. Only the PE stored in elastic deformation is returned on the recoil as coherent reverse motion of the nanosphere atoms. Capture occurs when the increased adhesion is able to overcome the weakened recoil motion.

Further monitoring of g demonstrated that, as in the case of bare Si nanospheres,[11] almost no β-tin phase exists in the end deposit. This is because under the nonequilibrium recoil conditions, the conical region undergoes a second phase change to an amorphous Si (a-Si) state. Although not themodynamically favorable, the trapped a-Si is favored here since this noncrystalline arrangement accommodates both with the unaffected upper spherical portion of the particle with cubic structure and the large contact, see last frame of Fig. 2(b).

In conclusion, our large-scale MD simulations showed that the poor reactivity of surfaces prevents the sticking of projectile H-passivated Si nanospheres. However, sticking is possible when speeds above 1000 m/s are attained. It is accompanied by the irreversible conversion of the incident energy into thermal agitation and by the occurrence of a phase transition, from diamond to β-tin, the latter eventually evolving to a-Si. These phase changes, also seen in the MD collision simulations with bare Si surfaces,[11] are not unrealistic. Although the considered impacting energies are relatively low and the nanosphere-substrate contact forces are not large, the nanosize extent of the contact zone renders p_m high enough to induce a first-order phase change. Indeed, both experimental and theoretical examinations of Si under pressure have revealed the existence of diverse crystalline phases other than cubic diamond. The first such phase is the β-tin state, which emerges under a pressure of 11 GPa.[20] More recently, the cubic to β-tin phase change was observed in Si nanocrystals during anvil experiments under a pressure of 22 GPa,[21] in good agreement with our data. The subsequent amorphization of the β-tin on the recoil is in contrast with the recovery of a metastable BC8 phase in bulk Si[22] but in agreement with the amorphization of the β-tin in Si nanocrystals after the release of the hydrostatic pressure.[21] The MD obtained succession of phase changes on a picosecond time scale is of interest for the fundamental understanding[23] of the transformation kinetics of solid phases in Si nanoparticles. More practically, the identified capture mediated by phase-transition plasticity improves our comprehension of the hypersonic plasma nanoparticle deposition experiments.[5]

We thank P. H. McMurry and S. L. Girshick for insightful discussions on the particle-reflection mode. Supported by NSF-NIRT Grant No. CTS-0506748. Calculations performed at the Minnesota Supercomputing Institute.

*Corresponding author. td@me.umn.edu

[1] R. E. Palmer, S. Pratontep, and H.-G. Boyen, Nat. Mater. **2**, 443 (2003).
[2] K. Wegner, P. Piseri, H. V. Tafreshi, and P. Milani, J. Phys. D **39**, 439 (2006).
[3] S. L. Girshick and J. Hafiz, J. Phys. D **40**, 2354 (2007).
[4] E. V. Johnson, G. Patriarche, and P. R. I. Cabarrocas, Appl. Phys. Lett. **92**, 103108 (2008).
[5] N. P. Rao, N. Tymiak, J. Blum, A. Neuman, H. J. Lee, S. L. Girshick, P. H. McMurry, and J. Heberlein, J. Aerosol Sci. **29**, 707 (1998).
[6] F. D. Fonzo, A. Gidwani, M. H. Fan, D. Neumann, D. I. Iordanoglou, J. Heberlein, P. H. McMurry, S. L. Girshick, N. Tymiak, and W. W. Gerberich, Appl. Phys. Lett. **77**, 910 (2000).
[7] W. W. Gerberich, W. M. Mook, C. R. Perrey, C. B. Carter, M. I. Baskes, R. Mukherjee, A. Gidwani, J. Heberlein, P. H. McMurry, and S. L. Girshick, J. Mech. Phys. Solids **51**, 979 (2003).
[8] K. Johnson, *Contact Mechanics* (Cambridge University Press, Cambridge, England, 1985).
[9] H. Ikeda, Y. Qi, T. Cagin, K. Samwer, W. L. Johnson, and W. A. Goddard, Phys. Rev. Lett. **82**, 2900 (1999).
[10] P. Valentini, W. W. Gerberich, and T. Dumitrică, Phys. Rev. Lett. **99**, 175701 (2007).
[11] P. Valentini and T. Dumitrică, Phys. Rev. B **75**, 224106 (2007).
[12] T. Hawa and M. R. Zachariah, Phys. Rev. B **71**, 165434 (2005).
[13] S. Ramalingam, D. Maroudas, and E. S. Aydil, J. Appl. Phys. **84**, 3895 (1998).
[14] J. Tersoff, Phys. Rev. B **37**, 6991 (1988).
[15] F. B. Mota, J. F. Justo, and A. Fazzio, J. Appl. Phys. **86**, 1843 (1999).
[16] R. Rurali and E. Hernandez, Comput. Mater. Sci. **28**, 85 (2003).
[17] H. Haberland, Z. Insepov, and M. Moseler, Phys. Rev. B **51**, 11061 (1995).
[18] H. Cheng and U. Landman, Science **260**, 1304 (1993).
[19] M. Kalweit and D. Drikakis, Phys. Rev. B **74**, 235415 (2006).
[20] J. Fameson, Science **39**, 762 (1983).
[21] S. H. Tolbert, A. B. Herhold, L. E. Brus, and A. P. Alivisatos, Phys. Rev. Lett. **76**, 4384 (1996).
[22] R. H. Wentorf and J. S. Kasper, Science **139**, 338 (1963).
[23] L. E. Brus, J. A. Harkless, and F. H. Stillinger, J. Am. Chem. Soc. **118**, 4834 (1996).